RAPID COMMUNICATIONS

PHYSICAL REVIEW B VOLUME 50, NUMBER 11 15 SEPTEMBER 1994-I

# Type-II→type-I transition in $(GaX)_n/(InX)_n$ (001) superlattices ($X$=P, Sb) as a function of period $n$

Alberto Franceschetti, Su-Huai Wei, and Alex Zunger
*National Renewable Energy Laboratory, Golden, Colorado 80401*
(Received 26 April 1994)

Coherently strained Ga$X$/In$X$ interfaces ($X$=P, Sb) lattice matched to a (001)-oriented substrate are predicted to have a type-I band-gap alignment, with both the valence-band maximum and the conduction-band minimum (CBM) located on the In-rich material. At the same time, the CBM wave function of short-period $(GaX)_n/(InX)_n$ superlattices is predicted to have larger amplitude on the Ga$X$ layers, leading to a type-II alignment. We show that (i) a type-II→type-I transition occurs around the period $n=4$; (ii) this transition has a different origin with respect to the well-known case of GaAs/AlAs superlattices; (iii) the band structure of ultrathin superlattices cannot be explained in terms of a simple effective-mass theory; (iv) the wave-function localization in short-period superlattices is determined by the atomic orbital energies.

In spite of the relatively large lattice mismatch between GaP and InP (7.4%), coherently strained $(GaP)_m/(InP)_n$ short-period superlattices ($m,n=1-4$) have been epitaxially grown on (001)-oriented GaAs substrates.[1,2] In addition to these *artificially* grown (001) superlattices, *spontaneous* (111) ordering occurs during vapor-phase growth of $Ga_{0.5}In_{0.5}P$ alloys, leading to CuPt-like $(GaP)_1/(InP)_1$ superlattices.[3] Despite these successful applications, very few results for GaP/InP valence-band offset (VBO) have appeared in the literature,[2,4–7] most of them[4–6] being theoretical predictions based on simple models. In this work, we use *ab initio* methods to calculate the VBO of coherently strained GaP/InP and GaSb/InSb heterojunctions. We find that when the heterojunction is lattice-matched to a (001)-oriented substrate whose lattice constant corresponds to the 50%-50% average of the binary compounds, both the valence-band maximum (VBM) and the conduction-band minimum (CBM) are located on the In-rich material. This result indicates that *long-period*, coherently strained Ga$X$/In$X$ (001) superlattices ($X$=P, Sb) will show a type-I (direct in real space) alignment. However, we also find that in *short-period* $(GaX)_n/(InX)_n$ (001) superlattices the $\Gamma$-like CBM wave function has larger amplitude on the Ga$X$ sublattice, while the VBM wave function is still localized on the In$X$ sublattice, leading to a type-II (indirect in real space) alignment. Therefore, a type-II→type-I transition is expected to occur as the period $n$ of the superlattice increases. Our calculations suggest that the crossover will take place at $n\simeq 4$ for GaP/InP superlattices and at $n\simeq 5$ for GaSb/InSb superlattices. This transition is qualitatively different from the well-known case of GaAs/AlAs, where the CBM of short-period, type-II superlattices has a strong $X$ character.[8] In Ga$X$/In$X$, on the other hand, the CBM wave function retains its $\Gamma$ character even in ultrathin superlattices. We show that this result is unexpected in the framework of a simple effective-mass theory, and propose a model that associates localization in ultrathin superlattices with *atomic orbital energies*. The basic rule that emerges is that when the CBM of a short-period superlattice originates mainly from the $\Gamma$ states of the binary constituents, its wave function is localized on the sublattice having deeper atomic $s$-orbital energy.

The VBO can be calculated[9] in a way which parallels its measurement in photoemission experiments by using core levels.[10] Denoting by $E_{\alpha,\mathrm{In}}$ and $E_{\beta,\mathrm{Ga}}$ the energies of the $\alpha$th core level of In and the $\beta$th core level of Ga, respectively, and by $E_{\mathrm{VBM}}$ the energy of the top of the valence band, the VBO between In$X$ and Ga$X$ can be written as

$$\Delta E_{\mathrm{VBM}}(GaX/InX)=(E_{\mathrm{VBM}}^{InX}-E_{\alpha,\mathrm{In}}^{InX})-(E_{\mathrm{VBM}}^{GaX}-E_{\beta,\mathrm{Ga}}^{GaX}) +(E_{\alpha,\mathrm{In}}^{GaX/InX}-E_{\beta,\mathrm{Ga}}^{GaX/InX}). \quad (1)$$

The first two bracketed terms give the binding energies of the $\alpha$th core level of In in epitaxially strained pure In$X$ and of the $\beta$th core level of Ga in epitaxially strained pure Ga$X$, respectively; the last bracketed term accounts for the core-level energy difference in the Ga$X$/In$X$ heterojunction. The sign of $\Delta E_{\mathrm{VBM}}(GaX/InX)$ is positive when the VBM of In$X$ is higher than that of Ga$X$. The VBO of a heterojunction depends on the strain state of the binary constituents and, through the third bracketed term in Eq. (1), on the chemistry and structure of the interface. If the binary constituents are grown pseudomorphically on a substrate, their strain state is determined by the substrate lattice constant $a_s$ and orientation $\mathbf{G}_s$. We take $a_s$ as the 50%-50% average of the calculated equilibrium lattice constants of Ga$X$ and In$X$ ($a_s$=5.67 Å for $X$=P and $a_s$=6.29 Å for $X$=Sb), and calculate $\Delta E_{\mathrm{VBM}}$ for $\mathbf{G}_s=(001)$ and $\mathbf{G}_s=(111)$. The biaxial strain in the plane of the substrate gives rise to a tetragonal distortion for (001)-oriented substrates, and to a trigonal distortion for (111)-oriented substrates; the strain in the direction perpendicular to the substrate and the cell-internal atomic positions are determined by minimizing the elastic energy with the valence-force-field method.[11] The band structures of the strained binary compounds are then calculated self-consistently using the linearized augmented plane wave method[12] in the local-density approximation (LDA).[13] The core levels are treated fully relativistically, while the valence states are calculated semirelativistically. The spin-orbit coupling of the valence states is included through a second variational procedure.[14] The core-level energy difference $\Delta E_{\mathrm{CL}}=E_{\alpha,\mathrm{In}}^{GaX/InX}-E_{\beta,\mathrm{Ga}}^{GaX/InX}$ is obtained from a self-

TABLE I. Theoretical predictions of the VBO of coherently strained, lattice-matched GaP/InP and GaSb/InSb heterojunctions, compared with the present results. The VBO is positive when the VBM of InP (InSb) is higher than that of GaP (GaSb). All values are in eV.

| | Present work | Van de Walle[a] | Cardona and Christensen[b] | Ichii *et al.*[c] | Armelles *et al.*[d] |
|---|---|---|---|---|---|
| GaP/InP (001) | 0.01 | 0.13 | −0.21 | −0.09±0.18 | 0.6 |
| GaP/InP (111) | 0.15 | 0.01 | −0.24 | | |
| GaSb/InSb (001) | 0.04 | 0.08 | −0.21 | −0.08±0.14 | |

[a]Reference 4.
[b]Reference 5.
[c]Reference 6.
[d]Reference 2.

consistent LDA calculation for a $(GaX)_n/(InX)_n$ strained-layer superlattice, using the same substrate lattice constant $a_s$ and orientation $\mathbf{G}_s$ as in the binary compounds. The convergence of $\Delta E_{CL}$ with the period $n$ of the superlattice has been checked: we find that for $n=4$ the convergence is better than 0.01 eV. For deep core levels, the energy $\Delta E_{CL}$ is nearly independent of the choice of the core levels, the typical difference being smaller than 5 meV.

Our results for the VBO's of coherently strained GaP/InP and GaSb/InSb heterojunctions are compared with previous calculations in Table I. For the most widely studied GaP/InP (001) interface, the previously calculated VBO's range between −0.2 eV (Ref. 5) and 0.6 eV;[2] we note, however, that these calculations are based on simplified models. Figure 1 depicts our calculated energy-level diagrams for the GaP/InP (001) and GaSb/InSb (001) heterojunctions. The threefold degenerate zinc-blende $\Gamma_{15v}$ state splits into $\Gamma_{6v}+\Gamma_{7v}^{(1)}+\Gamma_{7v}^{(2)}$, due to both crystal-field splitting and spin-orbit coupling. The VBM on the In$X$ side is $\Gamma_{6v}$, while the VBM on the Ga$X$ side is $\Gamma_{7v}^{(1)}$. The conduction-band states $X_{6c}^{z}$ and $X_{6c}^{x,y}$ are no longer degenerate in the strained binary, and the CBM of strained GaP is $X_{6c}^{z}$. As Fig. 1 demonstrates, both the VBM and the CBM of these (001) heterojunctions are located on the In-rich material, leading to a type-I band-gap alignment. While the centroid of the valence-band maximum is mainly affected by hydrostatic strain, biaxial strain has a large effect on crystal-field splitting, and therefore on the alignment of the VBM. For example, Hirakawa *et al.*[15] find that in the case of strained InAs grown on a GaAs substrate the VBM is on InAs (type-I), while for strained GaAs grown on the InAs the VBM is on GaAs (type-II). A similar behavior is expected for GaP/InP and GaSb/InSb heterojunctions.

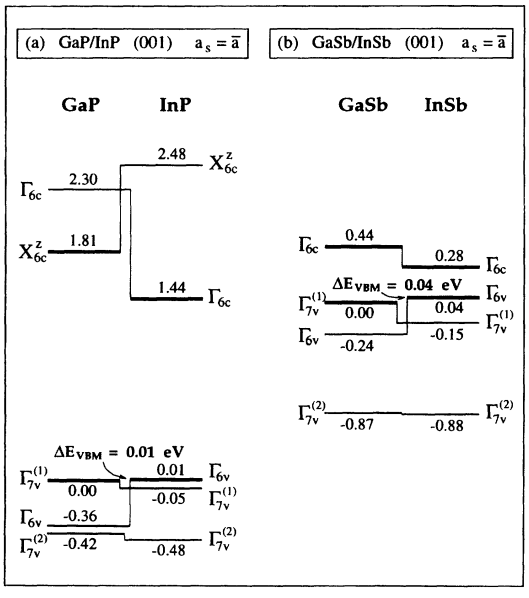


FIG. 1. Calculated energy levels (in eV) of coherently strained (a) GaP/InP (001) and (b) GaSb/InSb (001) heterojunctions. The substrate lattice constant $a_s$ is taken as the average of the binary constituents. Band gaps are corrected for the LDA error. The corrections for the $\Gamma_{6c}$ states (experimental band gap minus LDA band gap) are 1.31 eV for GaP, 1.00 eV for InP, 1.17 eV for GaSb, and 0.91 eV for InSb. The corrections for the $X_{6c}$ states are 0.77 eV for GaP and 0.71 eV for InP.

The wave-function localization in *long-period* superlattices is determined by the band offset between the binary constituents: the VBM wave function has larger amplitude on the material with higher VBM energy, while the CBM wave function has larger amplitude on the material with lower CBM energy. Therefore, according to Fig. 1, both the VBM and the CBM wave functions of long-period, lattice-matched Ga$X$/In$X$ (001) superlattices will be localized on the In-rich layers. As the period of the superlattice decreases, however, the superlattice band structure becomes more and more dominated by the coupling of states across the interfaces. In the limit of *short-period* superlattices the wave-function localization can no longer be related to the band lineup between the bulk binary constituents. This is illustrated in Fig. 2, which shows the wave-function amplitude of the band-edge states of monolayer GaP/InP (001) and GaSb/InSb (001) superlattices. We can see that in such ultrathin superlattices the CBM is more strongly localized on the Ga layer, while the VBM has a larger amplitude on the In layer, leading to a type-II alignment, whereby photoexcited electrons and holes are spatially separated. This type-II lineup has also been observed experimentally in short-period GaP/InP superlattices by Armelles *et al.*[2] From the temperature dependence of the Raman spectra, these authors conclude that in $(GaP)_2/(InP)_3$ and $(GaP)_3/(InP)_3$ superlattices grown on (001) GaAs substrates by molecular-beam epitaxy, electrons are localized on GaP while holes are localized on InP, in agreement with our results. We find a similar behavior in ultrathin GaP/InP (111) superlattices. This leads to an in-

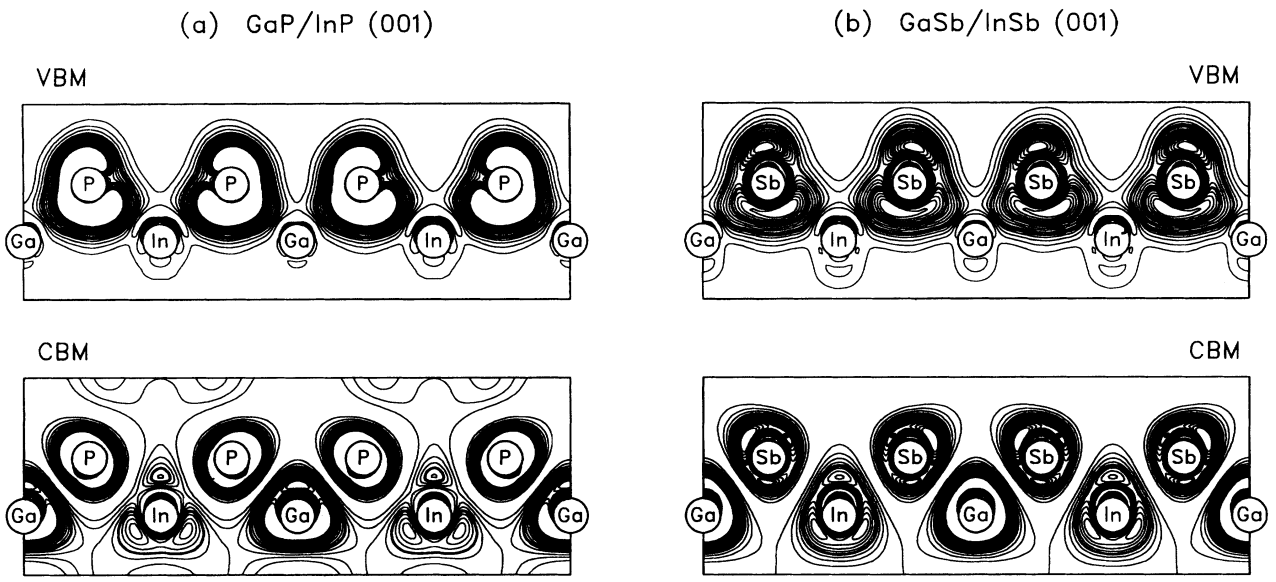


FIG. 2. Wave-function amplitudes $|\psi_i(\mathbf{r})|^2$ ($i$ is VBM, CBM) in the (011) plane of (a) $(GaP)_1/(InP)_1$ (001) and (b) $(GaSb)_1/(InSb)_1$ (001) superlattices. The contour step is 0.001 electrons/unit cell. Note that the VBM wave function has larger amplitude on In planes while the CBM wave function has larger amplitude on Ga planes.

teresting prediction: if a $Ga_xIn_{1-x}P$ system contains regions with just a few monolayers of strained GaP and InP (e.g., due to local phase separation of an alloy), then photoexcited electrons (holes) will exhibit spatial localization on GaP (InP).

The fact that long-period, coherently strained Ga$X$/In$X$ (001) superlattices are type-I (Fig. 1), while the corresponding short-period superlattices are type-II (Fig. 2), implies that a type-II–type-I transition should occur at some critical period $n_c$. This is borne out by the integrated wave-function amplitude $Q_i(R_\alpha)=\int_0^{R_\alpha}4\pi r^2\psi_i^2(r)dr$, where $i$ is the VBM and CBM states, around $\alpha$=Ga or In atoms. Figure 3 shows this quantity for $(GaP)_n/(InP)_n$ (001) superlattices as a function of the period $n$. We see that $Q_{CBM}$(Ga) decreases while $Q_{CBM}$(In) increases as the superlattice period $n$ increases. Since the charge inside a muffin-tin sphere depends on the choice of the muffin-tin radius $R_\alpha$, we estimate the type-II–type-I crossover by comparing the charges inside Ga and In spheres in the superlattice with the corresponding charges in the bulk strained compounds. We thus calculate that the type-II→type-I transition occurs around $n_c\simeq 4$ for $(GaP)_n/(InP)_n$ (001) superlattices and $n_c\simeq 5$ for $(GaSb)_n/(InSb)_n$ (001) superlattices.

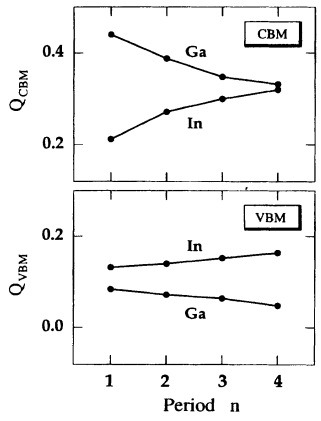


FIG. 3. Calculated VBM and CBM electronic charges enclosed in Ga and In muffin-tin spheres for $(GaP)_n/(InP)_n$ (001) superlattices, as a function of the period $n$. The muffin-tin radii are $R_{Ga}=1.18$ Å and $R_{In}=1.32$ Å. The electronic charge is normalized to 2 electrons/unit cell.

In order to explain the wave-function localization in short-period superlattices, we note that the band structure of the binary constituents does not provide a useful starting point. According to the predictions of a simple effective-mass model, the CBM of GaSb/InSb ultrathin superlattices should be still localized on InSb, while in GaP/InP ultrathin superlattices the CBM should have a strong $X$ character, because the InP $\Gamma$ CBM would be pushed above the GaP $X$ CBM by quantum confinement. Both these predictions contrast with our results. Instead, if the band-edge states of the superlattice originate from the zinc-blende $\Gamma$ states, *atomic orbital energies* provide a better indication of wave-function

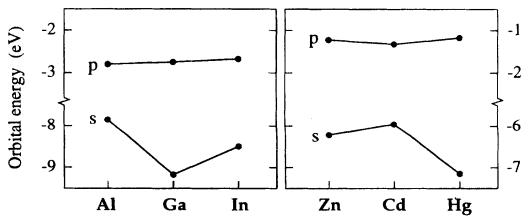


FIG. 4. Atomic orbital energies of neutral atoms calculated by the local-density approximation (Ref. 13).

localization. A reasonable rule for common-anion superlattices is that the Γ-like CBM will be localized on the cation sublattice with lower atomic $s$-orbital energy, while the Γ-like VBM will be localized on the cation sublattice with higher atomic $p$-orbital energy. The LDA calculated orbital energies of the Al, Ga, In, Zn, Cd, and Hg atoms are plotted in Fig. 4. As we can see, $\epsilon_{4s}(\mathrm{Ga}) < \epsilon_{5s}(\mathrm{In})$, and $\epsilon_{4p}(\mathrm{Ga}) < \epsilon_{5p}(\mathrm{In})$. Since the band-edge states of ultrathin $GaX/InX$ ($X$=P, As, or Sb) superlattices originate from the Γ states of the binary constituents, our rule predicts that the CBM will be localized on $GaX$, while the VBM will be localized on $InX$ (type-II alignment). This prediction is consistent with our explicit calculations for GaP/InP and GaSb/InSb systems, and with the results of Magri[16] for $(GaAs)_1/(InAs)_1$ (111) superlattices and of Taguchi and Ohno[17] for $(GaAs)_1/(InAs)_1$ (001) superlattices. These authors find that the CBM wave function of these systems has a larger amplitude on the GaAs layer. Our model predicts that in $GaX/AlX$ ($X$=P, As, Sb) short-period superlattices the VBM wave function and the Γ-like CBM wave function will be both localized on $GaX$, whereas in $InX/AlX$ superlattices the Γ-like band-edge states will be both localized on $InX$. Also, common-anion II-VI ultrathin superlattices are predicted to be type-I (see Fig. 4); this prediction is consistent with the results of Beavis *et al.*[18] for CdTe/HgTe superlattices.

In conclusion, we have shown that *atomic orbital energies* determine wave-function localization at the band edges of ultrathin ($n$=1–3), lattice-matched GaP/InP (001) and GaSb/InSb (001) superlattices, leading to a type-II alignment with the VBM on In and the CBM on Ga. On the other hand, as $n\to\infty$ we have a type-I heterojunction with both the VBM and the CBM localized on In. Thus, for these systems, a type-II→type-I transition of a novel type is expected as the period of the superlattice increases, and is predicted to occur around $n\simeq 4$. This result suggests that if we have some thin Ga-rich and In-rich domains in composition-modulated alloy,[19] then electrons will prefer Ga sites while holes will prefer In sites.

This work was supported by the U.S. Department of Energy, OER-BES, Grant No. DE-AC02-83-CH10093.

[1] R. M. Abdelouhab, R. Braunstein, M. A. Rao, and H. Kroemer, Phys. Rev. B **39**, 5857 (1989); M. I. Alonso, P. Castrillo, G. Armelles, A. Ruiz, M. Recio, and F. Briones, *ibid.* **45**, 9054 (1992).

[2] G. Armelles, M. C. Munoz, and M. I. Alonso, Phys. Rev. B **47**, 16 299 (1993).

[3] A. Gomyo, T. Suzuki, and S. Iijima, Phys. Rev. Lett. **60**, 2645 (1988).

[4] C. G. Van de Walle, Phys. Rev. B **39**, 1871 (1989).

[5] M. Cardona and N. E. Christensen, Phys. Rev. B **35**, 6182 (1987).

[6] A. Ichii, Y. Tsou, and E. Garmire, J. Appl. Phys. **74**, 2112 (1993).

[7] Y. Foulon and C. Priester, Phys. Rev. B **45**, 6259 (1992).

[8] S.-H. Wei and A. Zunger, J. Appl. Phys. **63**, 5794 (1988).

[9] S.-H. Wei and A. Zunger, Phys. Rev. Lett. **59**, 144 (1987).

[10] S. P. Kowalczyk, J. T. Cheung, E. A. Kraut, and R. W. Grant, Phys. Rev. Lett. **56**, 1605 (1986).

[11] P. N. Keating, Phys. Rev. **145**, 637 (1966); J. L. Martins and A. Zunger, Phys. Rev. B **30**, 6217 (1984).

[12] S.-H. Wei and H. Krakauer, Phys. Rev. Lett. **55**, 1200 (1985).

[13] P. Hohenberg and W. Kohn, Phys. Rev. **136**, B864 (1964); W. Kohn and L. J. Sham, *ibid.* **140**, A1133 (1965).

[14] A. H. MacDonald, W. E. Pickett, and D. D. Koelling, J. Phys. C **13**, 2675 (1980); W. E. Pickett, J. A. Freeman, and D. D. Koelling, Phys. Rev. B **23**, 1266 (1981).

[15] K. Hirakawa, Y. Hashimoto, K. Harada, and T. Ikoma, Phys. Rev. B **44**, 1734 (1991).

[16] R. Magri, Phys. Rev. B **41**, 6020 (1990).

[17] A. Taguchi and T. Ohno, Phys. Rev. B **36**, 1696 (1987).

[18] A. W. Beavis, M. Jaros, A. Zoryk, and I. Morrison, Semicond. Sci. Technol. **5**, 1051 (1990).

[19] K. A. Mäder and A. Zunger, Appl. Phys. Lett. **64**, 2882 (1994).